Pergamon

Free Radical Biology & Medicine, Vol. 17, No. 4, pp. 321–331, 1994
Copyright © 1994 Elsevier Science Ltd
Printed in the USA. All rights reserved
0891-5849/94 $6.00 + .00

0891-5849(94)E0054-M

Original Contribution

ELECTRON PARAMAGNETIC RESONANCE INVESTIGATIONS OF FREE RADICAL-INDUCED ALTERATIONS IN NEOCORTICAL SYNAPTOSOMAL MEMBRANE PROTEIN INFRASTRUCTURE

K. HENSLEY,*† J. CARNEY,‡ N. HALL,*† W. SHAW,* and D. A. BUTTERFIELD*†

*Department of Chemistry and †Center of Membrane Sciences, and ‡Department of Pharmacology, University of Kentucky, Lexington, KY, USA

(*Received* 13 *July* 1993; *Revised* 3 *November* 1993; *Re-revised* 17 *February* 1994; *Accepted* 22 *February* 1994)

Abstract—Evidence is presented that free radical stress can directly induce physico-chemical alterations in rodent neocortical synaptosomal membrane proteins. Synaptosomes were prepared from gerbil cortical brain tissue and incubated with 3 mM ascorbate and various concentrations of exogenous Fe^{2+} for 30–240 min at 37°C. Synaptosomes were then lysed and covalently labeled with the protein thiol-selective spin label MAL-6 (2,2,6,6-tetramethyl-4-maleimidopiperdin-1-oxyl) and subjected to electron paramagnetic resonance (EPR) spectrometry. In separate experiments, synaptosomal membranes were labeled with the thiol-specific spin label MTS ((1-oxyl-2,2,5,5-tetramethyl-pyrroline-3-methyl)-methanethiosulfonate), or the lipid-specific spin probe 5-NS (5-nitroxide stearate). Free radical stress induced by iron/ascorbate treatment has a rigidizing effect on the protein infrastructure of these membranes, as appraised by EPR analysis of membrane protein-bound spin label, but no change was detected in the lipid component of the membrane. These results are discussed with reference to potential oxidative mechanisms in aging and neurological disorders.

Keywords—Synaptosomes, Free radicals, EPR, Spin labeling, Aging, Alzheimer's disease

INTRODUCTION

A substantial body of evidence now exists to implicate reactive oxygen free radicals as contributors to the etiology of aging[1–3] and certain degenerative neurological disorders, particularly Parkinsonism, amyotrophic lateral sclerosis (ALS),[4] and Alzheimer's disease (AD).[5–7] There is also an increasing amount of data that correlates senile dementias, and to some degree normal aging, with disruption of central nervous system (CNS) and peripheral cell membrane structure and function.[8–10] However, researchers have only begun to investigate the potential link between free radical insult and neuronal membrane protein alteration.

Reactive oxygen free radicals have long been known to damage tissue through lipid peroxidation, protein cross-linking, and DNA cleavage processes, but the physiological significance of these phenomena remains unclear. Brain tissue is particularly sensitive to free-radical assault, partially because of its high content of oxidizable substrates (e.g., long chain fatty acids) and catalytically active metals (i.e., iron and copper). Relatively stable superoxide and hydrogen peroxide, which are produced by a variety of physiological pathways, react with trace amounts of iron or copper to form highly reactive hydroxyl free radicals (Fenton reactions):

$$\begin{aligned} O_2^{\cdot -} + Fe^{3+} &\rightarrow Fe^{2+} + O_2 \\ H_2O_2 + Fe^{2+} &\rightarrow {}^{\cdot}OH + OH^- + Fe^{3+} \\ \hline O_2^{\cdot -} + H_2O_2 + Fe^{2+,3+} &\rightarrow {}^{\cdot}OH + OH^- + O_2. \end{aligned}$$

The above mechanism is a simplified scheme, and does not consider the chelation state of the metal or competing reactions that may be pertinent in a biological milieu. Many reductants, such as ascorbate, can take the place of superoxide in the above scheme.

Data collected in our laboratory over a decade ago demonstrated breached membrane cytoskeletal protein

Address correspondence to: D. A. Butterfield, Dept. of Chemistry and Center of Membrane Sciences, University of Kentucky, Lexington, KY 40506, USA.

integrity and decreased cytoskeletal protein–protein interactions in erythrocytes taken from aged and AD donors, relative to young healthy controls.[8] Studies showing increased levels of spectrin breakdown products in aged and AD tissue may provide a theoretical framework for our early data.[9,10] Oxidative stress, produced in vivo or in vitro by hypoxia, ischemia–reperfusion, or by organic free radical-generating compounds, has been found to promote Ca^{2+} dependent proteolysis of high molecular weight cytoskeletal proteins in peripheral and CNS tissue, and concomitant reduction in electrophysiological parameters.[11–16] However, oxidative stress affects multiple aspects of cellular physiology; in particular, oxidative stress is known to release Ca^{2+} from internal stores[17,18] and to denature key regulatory enzymes.[19,20] Hence, reported membrane proteolysis and cytoskeletal disruption could be a secondary effect of the oxidation protocol. Indeed, there are data in the literature to suggest that oxidative stress increases erythrocyte membrane rigidity and mechanical stability as measured by ektacytometry.[21,22]

This paper reports a method that probes primary free radical-induced physico-chemical alterations occurring in the membrane protein architecture of purified neuronal synaptosomal suspensions. Gerbil neocortical synaptosomes were isolated, purified, and oxidized to various extents using an Fe^{2+}/ascorbate system, which mimics the Fenton chemistry thought to occur in vivo during oxidative stress. Synaptosomal membrane proteins were then covalently labeled using the protein thiol-selective spin label MAL-6 (2,2,6,6-tetramethyl-4-maleimidopiperdin-1-oxyl), which binds primarily to free protein –SH groups, or MTS ((1-oxyl-2,2,5,5-tetramethyl-pyrroline-3-methyl)-methanethiosulfonate), which is reported to bind exclusively to free protein thiols.[23,24] The membranes were then probed by electron paramagnetic resonance (EPR) spectrometry. This technique is sensitive to protein structural changes occurring in the spin-labeled substrate. Changes in the relevant parameters of the EPR spectra reflect changes induced in protein components of synaptosomal membrane during oxidative trauma, and suggest that oxidation has a rigidizing effect on the synaptosomal membrane protein infrastructure. In separate experiments, the lipid component of synaptosomal membranes was probed with the lipid-specific spin label 5-nitroxide stearate (5-NS). Analyses of the 5-NS spectra fail to indicate any oxidation-associated change in membrane fluidity.

MATERIALS AND METHODS

Chemicals

Ultra-pure sucrose used in synaptosome isolation was obtained from ICN Biochemicals. The protease inhibitors leupeptin, pepstatin, and aprotinin were obtained from Calbiochem. MTS was obtained from Reanal Chemicals, Budapest, Hungary. All other chemicals were obtained from Sigma Chemical Co. (St. Louis, MO) in the highest available purity.

Animals

Male Mongolian gerbils, 3 months of age, were obtained from Tumblebrook Farms (West Brookfield, MA) and subsequently housed in the University of Kentucky Central Animal Facility under 12 h light/dark conditions and fed standard Rodent Laboratory Chow (Purina) ad lib in the home cage. Animals were decapitated during the light phase, and the brain rapidly removed and placed on ice. The cortical mantle was dissected free, taking care to exclude the hippocampus and striatum, and the telencephalon was separated from underlying white matter. Cortices from 2–6 animals were then pooled and suspended in approximately 20 ml of ice-cold isolation buffer (0.32 M sucrose containing 4 μg/ml leupeptin, 4 μg/ml pepstatin, 5 μg/ml aprotinin, 20 μg/ml type II-S soybean trypsin inhibitor, 0.2 mM phenylmethylsulfonyl fluoride (PMSF), 2 mM ethylenediaminetetracetic acid (EDTA), 2 mM ethyleneglycolbistetracetic acid (EGTA), and 20 mM 4-(2-hydroxyethyl)-1-piperazineethanesulfonic acid (HEPES), and homogenized by 12 passes in a Wheaton 30 ml motor-driven Potter-type homogenizer with a Teflon pestle.

Synaptosome preparation

Synaptosomes were purified from homogenized cortices via ultracentrifugation across discontinuous sucrose gradients after the method of Ueda et al.[25] as adapted by Barnes[26] and further adapted in our laboratory.[27,28] Crude homogenate (in isolation buffer as described above) was centrifuged at 4°C, 1500 *g* for 10 min, the pellet discarded, and supernatant respun at 20,000 *g* for 10 min. The resulting pellet was carefully dispersed and this suspension layered on top of sucrose density gradients containing 12 ml each of 1.18 M sucrose, 1.0 M sucrose, and 0.85 M sucrose, plus 2 mM EDTA, 2 mM EGTA, and 10 mM HEPES (pH 8.0 for 0.85 M and 1.0 M sucrose solutions, pH 8.5 for 1.18 M solution). Samples were then spun at 4°C and 82,500 *g* for 120 min in an SW28 rotor in a Beckman L2-65B refrigerated ultracentrifuge. Synaptosomes were removed from the 1.18 M/1.0 M interface and the oxidation protocol executed. Experimental treatments were performed in duplicate on samples taken from the same synaptosome suspension.

Dose response study

Isolated synaptosomes were washed once in 10 volumes of oxidation buffer (10 mM HEPES, 137 mM NaCl, 4.6 mM KCl, 1.1 mM KH_2PO_4, 0.6 mM $MgCl_2$, and 1.1 mM EDTA, pH 7.4), centrifuged 10 min at 4°C and 20,000 *g*, and washed once more in the same buffer containing an additional 4 μg/ml leupeptin, 4 μg/ml pepstatin, 5 μg/ml aprotinin, and 0.2 mM PMSF. Total protein concentration was assayed by the method of Lowry[29] and adjusted to 7.0 mg/ml. Synaptosomal suspensions from each independent pool were split into duplicates for each treatment. Aliquots of synaptosomes were then dosed with small volumes of concentrated ascorbate (AA) (pH 7.4 in oxidation buffer), concentrated $FeSO_4$, and buffer to give a final protein concentration of 6.0 mg/ml, a final ascorbate concentration of 3 mM, and a desired Fe^{2+} concentration (0–300 μM in addition to endogenous iron). Iron and ascorbate solutions were prepared fresh immediately prior to use. Samples were then incubated in a water bath at 37°C for the desired length of time. Oxidation was stopped by addition to each sample of an equal volume of ice-cold 2 mM deferoxamine mesylate (pH 7.4 in oxidation buffer), followed immediately by centrifugation at 4°C in a table-top microcentrifuge and subsequent resuspension in lysing buffer (10 mM HEPES, 2 mM EDTA, and 2 mM EGTA, pH 7.4). All samples were then washed two more times in lysing buffer and spin labeled as described below.

Time course study

Synaptosomal suspensions were treated with 3 mM ascorbate and 3 μM or 30 μM Fe^{2+} as described above and allowed to incubate at 37°C in a water bath for various time periods (0, 30, 60, 120, and 240 min) before oxidation was terminated by addition of excess deferoxamine. After addition of deferoxamine, samples were immediately spun down and resuspended in 10–15 volumes of lysing buffer, and refrigerated at 4°C until all samples had been collected from the water bath. All samples were then washed two more times in lysing buffer and spin labeled as described below.

Spin labeling

MAL-6. Synaptosomes were lysed and subsequently washed twice in lysing buffer, then spin labeled for 18 h at 4°C in the presence of MAL-6 (20 μg MAL-6/mg protein, in lysing buffer). Samples were then centrifuged and washed 6 times in 10–15 volumes of lysing buffer to remove excess spin label. Samples were allowed to equilibrate to room temperature for 10 min prior to spectral acquisition. All spectra were obtained on a Bruker 300 EPR instrument equipped with computerized data acquisition and analysis capabilities (instrumental parameters: microwave frequency = 9.78 GHz, microwave power = 20 mW, modulation frequency = 100 KHz, modulation amplitude = 0.30 G, time constant = 1.28 ms). The relevant spectral parameter (W/S ratio) was averaged for each duplicate pair of samples.

MTS. Synaptosomes were lysed and subsequently washed twice in lysing buffer, then spin labeled by incubating for 30 min at room temperature in the presence of MTS (20 μg MTS/mg protein in lysing buffer). Samples were then washed and spectroscopically analyzed as described above.

5-*NS.* 0.25 ml of the spin probe dissolved in chloroform was deposited in a borosilicate culture tube, and evaporated under N_2. 0.5 ml of lysed, washed synaptosomes were added to the 5-NS tubes to give a final protein concentration of about 3 mg/ml and a 5-NS:lipid ratio of approximately 1:40. Samples were incubated at room temperature, with gentle agitation, for 30 min. Spectroscopic analysis was performed as described above.

DTNB assay for thiols; electrophoretic separations

Total thiol content of synaptosomal membranes was determined colorimetrically by the urea-based method of Sedlak and Lindsay,[30] which monitors the thiol-induced decomposition of 5,5′-dithiobis-(2-nitrobenzoic acid) (DTNB) into nitromercaptobenzoate (A_{max} = 412 nm). Samples were calibrated against cysteine standards, and care was taken to prepare appropriate sample and reagent blanks to subtract background absorbance.

Gel electrophoresis was perfomed according to the method of Laemmli,[31] using 3.6%/4.8% and 5%/12% stacking gel/separating gel acrylamide concentrations.

Data analysis

Data was analyzed by two-tailed Student's *t*-test. A value of $p < 0.05$ was considered statistically significant.

RESULTS

Relevant spectral parameters

MAL-6: *W/S ratio.* A typical EPR spectrum of MAL-6 covalently attached to membrane proteins in cortical

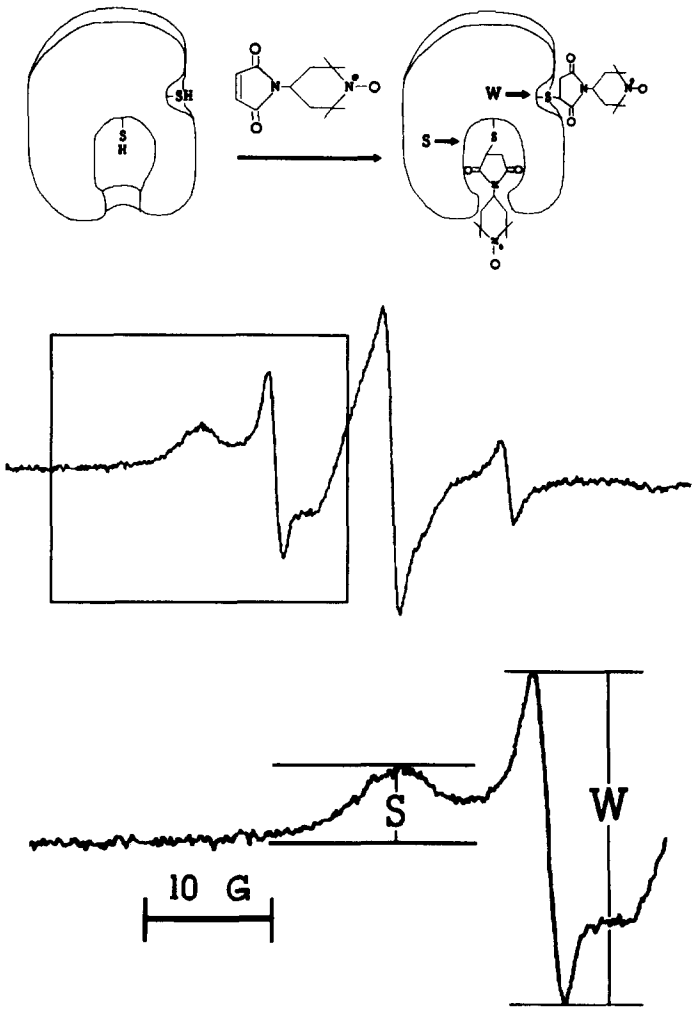

Fig. 1. Selective spin labeling of membrane protein cysteine −SH groups by MAL-6. (Top) schematic diagram of hypothetical protein (cross-section) showing weakly (W) and strongly (S) immobilized binding sites. (Middle) Typical EPR spectrum of MAL-6 labeled rodent synaptosomes. (Bottom) The low-field, $M_I = +1$ EPR resonance lines showing W and S components.

synaptosomes is shown in Fig. 1. At least two distinct populations of spin label binding sites, characterized by their ability to restrict spin label motion, are observed. The relevant EPR parameter measured is the ratio of the spectral amplitude of the $M_I = +1$ low-field weakly immobilized line (W) and that of the $M_I = +1$ low-field strongly immobilized line (S), which is referred to as the W/S ratio (Fig. 1). Changes in the W/S ratio are known to be strong indicators of perturbations in the normal interactions of cytoskeletal proteins.[32–40] An increase or decrease in the W/S ratio is conceptualized as arising from protein structural changes that decrease or increase, respectively, the steric hindrance to segmental motion in the region of protein to which the spin label is attached (Fig. 1). Experiments designed to decrease cytoskeletal protein–protein interactions in erythrocytes (via treatment with polyanions or mild proteolysis) are characterized by an increase in the W/S ratio of erythrocyte cytoskeleton-bound MAL-6[34,35] resulting from increased motion of the spin label. In contrast, treatments that are known to strengthen protein–protein interactions in erythrocytes (addition of polycations or crosslinking agents) are observed to cause a decrease in the W/S ratio.[36,37] Synaptosomal membranes possess analogs of most major erythrocyte cytoskeletal and transmembrane proteins, including spectrin, ankyrin, and band 3, and data from our laboratory employing protein crosslinkers, proteases, and potential AD therapeutic agents[38–40] indicate that the above-described W/S correlations from erythrocyte studies are generalizable to synaptosomes as well.

MTS: Apparent rotational correlation time τ_a. It

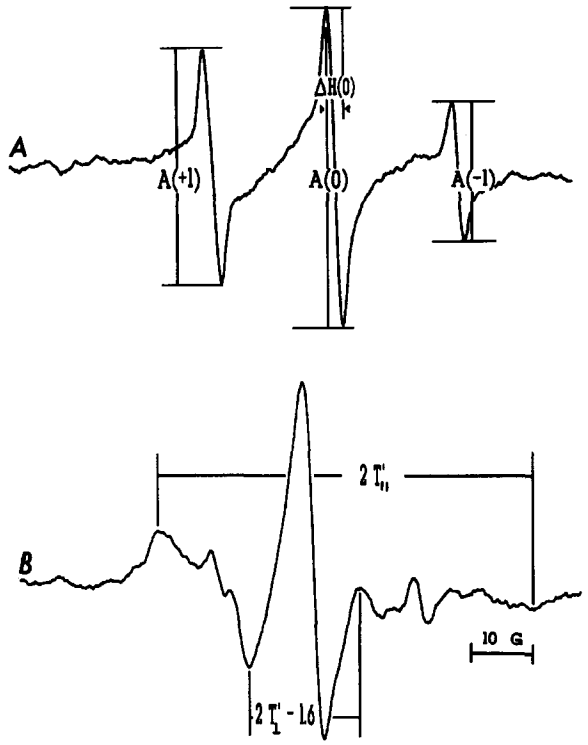

Fig. 2. (A) Typical spectrum of MTS labeled (untreated) synaptosomal membrane proteins, showing parameters used in calculation of the apparent rotational correlation time τ_a. (B) Typical spectrum of 5-NS labeled synaptosomal membrane lipids, showing parameters used in calculation of the order parameter S.

should be noted that, unlike MAL-6, MTS behavior has not been thoroughly characterized in the synaptosomal membrane system. Under the labeling conditions employed in this study, no accurate W/S parameter is extractable from the MTS spectra of unoxidized synaptosomal membranes, as there is no clearly defined S component of the $M_I = +1$ resonance line. Motional restriction of the spin label must, in this case, be deduced from the MTS spectra by calculation of apparent rotational correlation times (τ_a). The τ_a parameter is calculated from the equation:

$$\tau_a(s) = 6.5 \times 10^{-10} H(0) \times \left[\sqrt{\left(\frac{A(0)}{A(+1)}\right)} + \sqrt{\left(\frac{A(0)}{A(-1)}\right)} - 2\right],$$

where $H(0)$ is the peak-to-peak linewidth of the $M_I = 0$ central line and $A(n)$ refers to the peak-to-peak amplitudes of the $M_I = +1, 0$, or -1 lines[41] (Fig. 2A). τ_a can be thought of as the time required for a spin label to complete rotation through one radian in space. An increase in τ_a represents increased hindrance to spin label motion.[33-36]

5-NS: Order parameter S. The amphipathic spin probe 5-NS is thought to intercalate within both halves of a lipid bilayer so that its long alkyl chain is roughly parallel with the alkyl chains of membrane lipids, and its paramagnetic nitroxide is near the lipid/aqueous interface.[33,42] In this model, rapid anisotropic motion occurs about the long axis of the spin probe, which engenders new effective T tensor elements $T'_\parallel$ and $T'_\perp$. An order parameter S can be calculated from these T-tensor values by the equation:

$$S = \frac{T'_\parallel - T'_\perp}{T_\parallel - T_\perp} * \frac{TrT}{TrT'}$$

$$TrT' = T'_\parallel + 2T'_\perp,$$

where the primed values are spectroscopically measured (Fig. 2B) and the unprimed values are known constants obtained from single crystal data.[42] An increase in S is taken to indicate a decrease in the fluidity of the lipid microenvironment about the spin probe.[33]

Fe^{2+} *dose response (MAL-6)*

The W/S ratio of MAL-6 labeled synaptosomes incubated 30 min at 37°C was approximately 10% lower than that of samples held at 4°C, even in the absence of added prooxidants (mean ± standard deviation (SD) of heated samples = 90.7% ± 10.7% of unheated controls, $N = 11$, $p < 0.02$). For this reason the data in this study (Fig. 3) are displayed as percent of control values taken from synaptosomes incubated at 37°C in the absence of exogenous prooxidants.

In the absence of added ascorbate, addition of iron loads up to 300 μM causes a small and statistically insignificant decrease in the W/S ratio (mean decrease of 3.8% ± 4.8% SD, $N = 4$). Ascorbate (3 mM) causes a small decrease in this EPR parameter even in the absence of exogenous iron (2.3% ± 0.8% SD, $N = 4$, $p < 0.02$), presumably as a result of endogenous iron or copper ion present. However, iron and ascorbate, when incubated together with the synaptosomal suspension, interact to produce a synergistic effect, decreasing the W/S ratio up to 15% from the 37°C control in an Fe^{2+} concentration-dependent manner over three orders of magnitude in Fe^{2+} (Fig. 3). Figure 3 is plotted using semilogarithmic axes. If the data are plotted on Cartesian axes, it is observed that the W/S ratio decreases linearly in a statistically significant manner

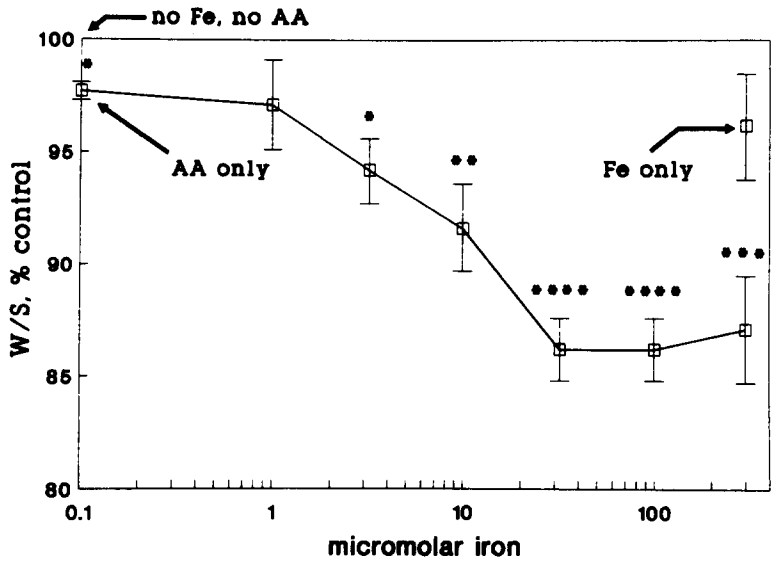

Fig. 3. Effect of oxidative stress on W/S ratio of MAL-6 labeled synaptosomes. All points on the curve represent synaptosomes incubated with 3 mM ascorbate, 37°C, 30 min with variable Fe^{2+} as described in the text. "Fe^{2+} only" indicates samples incubated in 300 μM Fe^{2+}, zero ascorbate. "AA only" indicates samples incubated in 3 mM ascorbate, zero exogenous iron. All data expressed as percent coincubated control (no iron or ascorbate) ± standard error about the mean. *$p < 0.006$; **$p < 0.004$; ***$p < 0.002$; ****$p < 0.0002$. $N = 4–6$ samples for each data point.

with increasing iron loads up to approximately 30 μM exogenous iron (in the presence of 3 mM ascorbate). Above this concentration the W/S response begins to plateau.

Extrapolation of percent change in W/S ratio from the 37°C control vs. concentration of added iron through the linear region below 30 μM exogenous Fe^{2+} (Fig. 4), yields an intercept on the abscissa indicative of the initial "endogenous" iron concentration (plus, possibly, a contribution from trace amounts of copper, which would be indistinguishable from iron in this case). This value, putatively representing endogenous synaptosomal iron (but not completely exluding trace amounts of iron in the buffer, which was determined by atomic absorption to be less than 1 μM (data not shown)), was estimated to be approximately 0.064 μg Fe^{2+}/mg protein

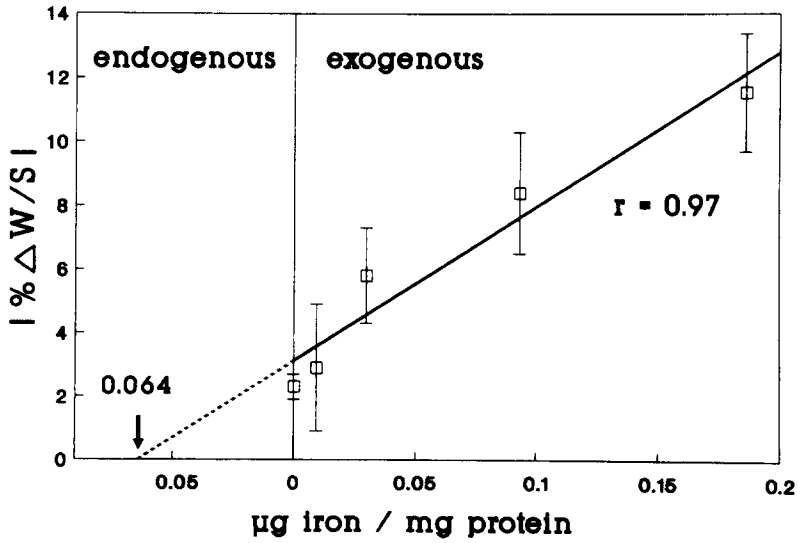

Fig. 4. Change in W/S ratio with increasing Fe^{2+}/protein ratio (linear range). Arrow indicates putative endogenous iron concentration of 0.064 μg/mg protein. Error bars indicate standard error about the mean.

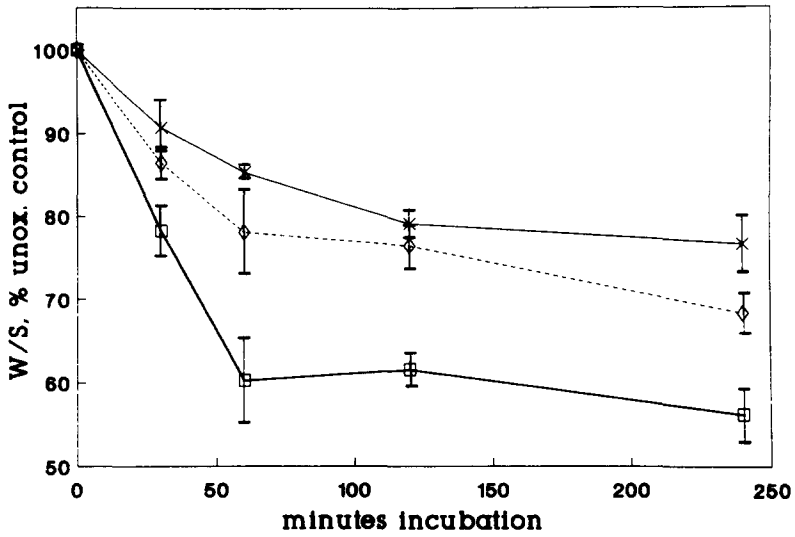

Fig. 5. Time course of oxidative stress. (x) = synaptosomes incubated without exogenous iron or ascorbate; (◇) = synaptosomes incubated at 37°C with 3 mM ascorbate and 3 μM Fe^{2+}; (□) = synaptosomes incubated at 37°C with 3 mM ascorbate and 30 uM Fe^{2+}. Data expressed as percent unoxidized controls (kept at 4°C, no added prooxidants). Error bars indicate standard error about the mean. N = 4–6 samples per data point.

(6.9 μM at 6 mg/ml protein). Rodent brain iron concentrations of about 0.074 μg/mg protein have been previously determined by atomic absorption/atomic emission techniques.[43–45] The agreement between our extrapolated "endogenous" iron level and accepted values, lends confidence to the EPR measurements reported in this study.

Time course study (MAL-6)

The controls in Fig. 3 are samples heated at 37°C for 30 min in the absence of added Fe^{2+} and ascorbate. To illustrate the effect of prolonged incubation time upon the W/S ratio of spin-labeled synaptosomes exposed to different levels of oxidative stress, the controls in Fig. 5 are samples held at 4°C in the absence of prooxidants. As before, we observed a decrease of the W/S ratio in response to 37°C incubation, in the absence of exogenous prooxidants (Fig. 5, uppermost curve). Addition of 3 mM ascorbate and 3 μM Fe^{2+} or 30 μM Fe^{2+} (Fig. 5, lower two curves, respectively) produces an additive decrease in the W/S ratio beyond the effect induced solely by heating (i.e., 1 h incubation with 3 mM ascorbate and 0 μM, 3 μM, or 30 μM Fe^{2+} leads to reduction in the W/S ratio of MAL-6 of approximately 10, 20, and 40%, respectively).

Oxidation—associated alteration in MTS, 5-NS spectra

Table 1 summarizes the effect of extreme oxidative stress (300 μM Fe^{2+}, 3 mM AA, 30 min incubation at 37°C) on the apparent rotational correlation time of MTS labeled membrane proteins and the order parameter of 5-NS probed membranes.

The spectra of MTS labeled membrane proteins showed qualitative as well as quantitative changes as a result of oxidation (Fig. 6). In particular, MTS spectra from oxidized membranes showed a clearly defined $M_I = +1$ strongly immobilized component similar to (but much weaker than) that seen in MAL-6 labeled samples. No such component was present in controls. The linewidth of the $M_I = +1$ weakly immobilized component also broadened noticeably upon treatment with Fe^{2+}/AA (Fig. 6). Heating at 37°C induced an increase in τ_a of approximately 9% relative to controls held at 4°C. Fe^{2+}/AA treatment caused an additional 15% increase in τ_a (Table 1) .

Analysis of 5-NS probed membranes showed no

Table 1. Comparison of Spectral Parameters from 5-NS and MTS Labeled Synaptosomes Subjected to Incubation at 37°C With and Without Fe^{2+}/AA Induced Oxidation; Values Relative to Controls Maintained at 4°C With No Exogenous Prooxidants

	5-NS: Mean % ΔS (p-value)	MTS: Mean % $\Delta\tau_a$ (p-value)
37°C, 30 min, no Fe^{2+}/AA	0.9 (ns)	9.3 (0.092)
37°C, 30 min, 300 μM Fe^{2+}/3 mM AA	2.8 (ns)	24.8 (0.034)

N = 5 for each treatment; ns = not significant above 90% confidence interval.

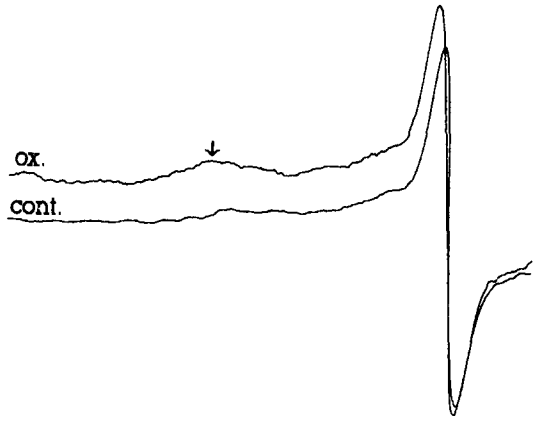

Fig. 6. Expansion of $M_I = +1$ low-field line of MTS labeled synaptosomal membrane proteins subjected to oxidative stress as described in the text (top) compared to controls (bottom). Arrow indicates strongly immobilized component that appears after iron/ascorbate treatment.

change in the order parameter as a result of heating or Fe^{2+}/AA treatment (Table 1).

Controls for proteolysis, thiol oxidation; nonmembrane effects

Oxidized (300 μM Fe^{2+}, 3 mM AA, 37°C, 30 min) synaptosomal membranes bound significantly less MAL-6 than did unoxidized (heated, no added prooxidants) samples, as assessed by double integration of the entire EPR spectra (mean MAL-6 binding to oxidized samples as percent of unoxidized control = 66.8 ± 25.64 SD, $N = 11$, $p < 0.002$). Given these data, we investigated the possibility that proteolysis and/or thiol crosslinking were destroying potential MAL-6-SH sites.

DTNB assays performed on synaptosomal membranes showed no significant difference between free thiol content of oxidized (300 μM Fe^{2+}, 3 mM AA, 30 min at 37°C) and unoxidized samples (30 min, 37°C, no added prooxidants) (data not shown).

Synaptosomal proteins can be separated and visualized by SDS-PAGE using either a 3.6%/4.8% Laemmli discontinuous gel system (for proteins of about 90 kD to about 250 kDa) or a 5%/12% system (for proteins of about 15 kD to about 90 kD). Polyacrylamide gel profiles of unoxidized (unheated, no exogenous Fe^{2+}/AA) and oxidized (37°C, 30 min, 300 μM Fe^{2+}, 3 mM AA) synaptosomal samples did not differ in any obvious qualitative manner, regardless of whether the gels were electrophoresed under reducing (with 10% β-mercaptoethanol in sample buffer) or nonreducing (without β-mercaptoethanol) conditions (data not shown). The oxidation protocol was also executed with omission of protease inhibitors from the oxidation buffer. This did not noticeably affect the magnitude or direction of the W/S ratio change that accompanied 37°C heating or Fe^{2+}/AA treatment (data not shown). To rule out any artifacts stemming from nonmembrane bound components within the synaptosomes, we oxidized lysed, washed synaptosomal membranes and observed the same decrease in the W/S ratio seen in the unlysed samples (data not shown).

DISCUSSION

Synaptosomes isolated from brain tissue retain many of the morphological and functional characteristics of the nerve terminal.[28,46] Though the architecture of the neuronal cytoskeleton has not been as thoroughly mapped as that of the erythrocyte, it is generally thought that the synaptic cortex has a membrane skeleton similar to those found in erythrocytes and other peripheral tissues.[27,38] Electron microscopic studies have shown that in our hands the synaptosomal suspensions produced by sucrose density gradient centrifugation have only an occasional contribution of nonsynaptic inclusions, such as mitochondria and microsomes,[28] and EPR characterization experiments have shown that MAL-6 labels synaptosome membrane-associated proteins exclusively in this system.[27,28]

The data presented in this paper show that in vitro generation of free radicals by means of an iron/ascorbate system produces a characteristic alteration in the synaptosomal membrane protein infrastructure as judged by EPR analysis. The W/S ratio of MAL-6 labeled synaptosomes, oxidatively stressed by contact with Fe^{2+}/AA, was found to be reduced relative to the W/S ratio of unoxidized controls (or, more precisely, less oxidized controls, because some unintentional oxidation is inevitable). This decreased W/S ratio is suggestive of increased protein–protein interactions and/or conformational compactions in the microenvironment of the spin probes, which increase the steric hinderance and decrease the segmental motion of protein-bound MAL-6. Experiments utilizing a second, thiol-specific spin label (MTS) corroborate the MAL-6 results; the observed increase in τ_a upon heating or Fe^{2+}/AA addition closely parallels the decrease in W/S ratio for the same treatments, and the de novo appearance of an $M_I = +1$ low-field resonance peak in the MTS spectra of oxidized synaptosomes is completely consistent with this interpretation. Our synaptosome EPR data are consistent with previously published ektacytometric observations[21,22] of increased membrane rigidity in erythrocytes undergoing oxidative insult.

The observed decrease in spectral intensity of MAL-6 bound to previously oxidized membranes further supports an interpretation of increased steric hindrance about MAL-6 binding sites. Conformational changes in a protein that "tightens" the local protein structure in the vicinity of spin label binding sites are known to decrease the rate of reaction of protein with spin labels.[47] The binding site of the protein simply becomes less accessible to the spin probe. Other researchers have recently described reduced binding of the maleimide fluorochrome DACM (*N*-(7-dimethyl-amino-4-methyl-coumarinyl) maleimide) to membrane proteins taken from aged erythrocytes, and have interpreted their data to indicate oxidatively induced conformational compaction of aged proteins and decreased accessibility of labeling sites.[48,49] Our synaptosomal EPR data are consistent with this pattern seen in erythrocyte studies. Because we found no significant difference between nonreducing gel profiles or free −SH content of oxidized and unoxidized synaptosomes, it seems unlikely that the reduced MAL-6 incorporation is attributable to simple thiol oxidation. Nor is it likely that our data result from secondary alterations in the physical state of bilayer lipids, because the EPR spectra of the lipid specific spin label 5-NS showed no differences between oxidized and control samples.

The observed W/S ratio decrease and τ_a increase, upon heating, even in the absence of prooxidants, is probably best explained as a phenomenon independent of oxidation. Incubation at 37°C for 30 min (no added iron or ascorbate) decreases the W/S ratio about 10% relative to unheated samples; the maximum decrease inducible via our oxidation protocol within this time period is about 25–30% below unheated samples. If the 10% decrease is due to reactive radicals generated from "endogenous iron" (about 7 μM) in the absence of ascorbate, then heating in the presence of 300 μM exogenous iron should produce a much larger decrease. This is not the case (Fig. 3). We therefore speculate that the observed decrease in the W/S ratio of MAL-6 labeled synaptosomes upon heating (no exogenous prooxidants) is due mainly to cytoskeletal protein conformational rearrangements independent of free-radical mediated phenomena.

Our data are not consistent with the disruptive membrane alterations that some other researchers have observed to accompany cellular oxidative stress. However, our system differs from these models in several ways. First, our synaptosome system is much simpler and considerably more homogeneous than systems involving whole tissue, multiple cell types, or crude brain homogenates. Oxidative stimuli applied to such complex mixtures could affect component cell membranes via multiple, possibly antagonistic, pathways. Second, systems utilizing phenylhydrazine, menadione, etc. as a radical generator may affect response variables through nonoxidative interaction of these drugs with the cell membrane or other cellular components. The iron/ascorbate system can be manipulated to control for possible nonoxidative interactions, simply by omitting ascorbate or iron and verifying that the remaining component has no independent effect on the response variable. It should also be noted that the synaptosome isolation protocol we employed involves early chelation of Ca^{2+} via EGTA; Ca^{2+}-dependent proteolysis was therefore hindered. There is a possibility that primary changes in protein conformation, induced by direct oxidation, may predispose a protein to subsequent processing. Hence, our synaptosome results may complement, rather than contradict, previous studies done in more complex and less well-defined systems.

This paper presents evidence, from two separate protein-specific spin labels, that free radical stress can directly induce physico-chemical alterations in rodent synaptosome membrane proteins. Free radical stress induced by iron/ascorbate treatment may have a rigidizing effect on the protein infrastructure of these membranes, as judged by EPR analysis of membrane-bound protein-specific spin labels. Gross alteration of membrane protein structure conceivably could alter membrane function as well, ranging from alterations in ion flux,[50] to increased susceptibility to IgG binding,[51,52] and potentially altered proteolysis of transmembrane proteins.[53,54] Further research into the effects of free radical-induced stress on neuronal membrane protein integrity may provide mechanistic interpretations for the putative correlation between imbalanced oxidative homeostasis and physiological/cognitive abnormalities.[55] Such studies are currently underway in our laboratory.

Acknowledgements—This work was supported in part by grants from NIH (AG-10836) and NSF (EHR-9108764). K. H. is a a recipient of an Office of Naval Research Graduate Fellowship.

REFERENCES

1. Harman, D. The ageing proces. *Proc. Natl. Acad. Sci. USA* **78:**7124–7128; 1981.
2. Carney, J. M.; Starke-Reed, P. E.; Oliver, C. N.; Landum, R. W.; Cheng, M. S.; Wu, J. F.; Floyd, R. A. Protection against oxidative damage to CNS by alpha-phenyl-tert-butyl nitrone (PBN) and other spin-trapping agents: A novel series of nonlipid freeradical scavengers. *Proc. Natl. Acad. Sci. USA* **88:**3633–3636; 1991.
3. Cutler, R. G. Antioxidants and longevity of mammalian species. In: Woodhead, A.D; Blackett, A.D; Hollaender, A, eds. *Molecular biology of aging.* New York: Plenum Press; 1985:15–56.
4. Rosen, D. R.; Siddique, T.; Patterson, D.; Figlewicz, D. A.;

Sapp, P.; Hentati, A.; Donaldson, D.; Goto, J.; O'Regan, J. P.; Deng, H. X. Mutations in Cu/Zn superoxide dismutase gene are associated with familial amyotrophic lateral sclerosis. *Nature* **362:**59–62; 1993.
5. Role of iron and oxidant stress in the normal and Parkinsonian brain. *Annals of Neurology*, **32s:**1–145; 1992.
6. Swaab, D. F. Brain ageing and Alzheimer's disease, "wear and tear" vs. "use it or lose it." *Neurobiology of Ageing* **12:**317–324; 1991.
7. Blass, J. P.; Gibson, G. E. The role of oxidative abnormalities in the pathophysiology of Alzheimer's disease. *Rev. Neurol.* (Paris) **147:**513–525; 1991.
8. Markesbery, W. R.; Leung, P.K.; Butterfield, D. A. Spin label and biochemical studies of erythrocyte membranes in Alzheimer's disease. *J. Neur. Sci.* **45:**323–330; 1980.
9. Bahr, B. A.; Vanderklish, P. W.; Ha, L. T.; Tin M. T.; Lynch, G. Spectrin breakdown products increase with age in telencephalon of mouse brain. *Neuroscience Lett.* **131:**237–240; 1991.
10. Peterson, C.; Vanderklish, P.; Seubert, P.; Cotman, C.; Lynch, G. Increased spectrin proteolysis in fibroblasts from aged and Alzheimer's donors. *Neurosci. Lett.* **121:**239–243; 1991.
11. Oliver, M.; Baudry, M.; Lynch, G. The protease inhibitor leupeptin interferes with the development of long-term potentiation in hippocampal slices. *Brain Res.* **505:**233–238; 1989.
12. Arduini, A.; Storto, S.; Belfiglio, M.; Scurti, R.; Mancinelli, G.; Federici, G. Mechanism of spectrin degradation induced by phenylhydrazine in intact human erythrocytes. *Biochim. Biophys. Acta* **979:**1–6; 1989.
13. Mortensen, A. M.; Novak, R. F. Enhanced proteolysis and changes in membrane-associated calpain following phenylhydrazine insult to human red cells. *Tox. App. Pharm.* **110:**435–449; 1991.
14. Arai, A.; Vanderklish, P.; Kessler, M.; Lee, K.; Lynch, G. A brief period of hypoxia causes proteolysis of cytoskeletal proteins in hippocampal slices. *Brain Res.* **555:**276–280; 1991.
15. Arai, A.; Kessler, M.; Lee, K.; Lynch, G. Calpain inhibitors improve the recovery of synaptic transmission from hypoxia in hippocampal slices. *Brain Res.* **532:**63–68; 1990.
16. Caprari, P.; Bozzi, A.; Ferroni, L.; Strom, R.; Salvati, A. M. Oxidative erythrocyte membrane damage in hereditary spherocytosis. *Biochem. International* **26:**265–274; 1992.
17. Hermes-Lima, M.; Castilho, R. F.; Valle, V. G. R.; Bechara, E. J. H.; Vercesi, A. E. Calcium-dependent mitochondrial oxidative damage promoted by 5-aminolevulinic acid. *Biochim. Biophys. Acta* **1180:**201–206; 1992.
18. Richter, C.; Balz, F. Ca^{2+} movements induced by hydroperoxides. In: Woodhead, A. D; Blackett, A. D.; Hollaender, A. *Molecular biology of aging.* New York: Plenum Press; 1985:221–241.
19. Fucci, L.; Oliver, C. N.; Coon, M. J.; Stadtman, E. R. Inactivation of key metabolic enzymes by mixed-function oxidation reactions: Possible implication in protein turnover and ageing. *Proc. Natl. Acad. Sci. USA* **80:**1521–1525; 1983.
20. Stadtman, E. R. Metal ion-catalyzed oxidation of proteins: Biochemical mechanism and biological consequences. *Free Radic. Biol. Med.* **9:**315–325; 1990.
21. Kuypers, F. A.; Scott, M. D.; Schott, M. A.; Lubin, B.; Chiu, D. T. Use of ektacytometry to determine red cell susceptibility to oxidative stress. *J. Lab. Clin. Med.* **116:**535–45; 1990.
22. Hebbel, R. P.; Leung, A.; Mohandas, N. Oxidation-induced changes in microrheologic properties of the red cell membrane. *Blood* **76:**1015–1020; 1990.
23. Berliner, L. J.; Greenwald, J.; Hankovsky, H. O.; Hideg, K. A novel thio-specific spin label: Papain active site labeling and inhibition. *Analyt. Biochem.* **119:**450–455; 1982.
24. Butterfield, D. A.; Lee, J.; Ganaparthi, S.; Bhattacharyya, D. Biofunctional membranes: Part IV: Active site structure and stability of an immobilized enzyme, papain, on modified polysulfone membranes studied by electron paramagnetic resonance and kinetics. *J. Membr. Sci.* in press; 1994.
25. Ueda, T.; Greengard, T.; Berzins, K.; Cohen, R. S.; Blomberg, F.; Grab, D. G.; Siekevitz, P. Subcellular distribution in cerebral cortex of two proteins phosphorylated by a cAMP-dependent protein kinase. *J. Cell Biol.* **83:**308–319; 1979.
26. Barnes, G. *The role of Ca^{2+}-dependent kinases and phosphatase 2A in the kindling model of epilepsy.* Ph.D. Thesis, University of Kentucky; 1991.
27. Umhauer, S. A.; Isbell, D. T.; Butterfield, D. A. Spin labeling of membrane proteins in mammalian brain synaptic plasma membranes: Partial characterization. *Analyt. Letts.* **25:**1201–1215; 1992.
28. Umhauer, S. *Spin labeling of membrane proteins in mammalian brain synaptic plasma membranes: Partial characterization and relevance to aging and Alzheimer's disease.* Ph.D. Thesis, University of Kentucky; 1992.
29. Lowry, O. H.; Rosebrough, N. J.; Farr, A. L.; Randall, R. J. Protein measurement with the Folin phenol reagent. *J. Bio. Chem.* **193:**265–275; 1951.
30. Sedlak, J.; Lindsay, R. H. Estimation of total, protein-bound and nonprotein sulfhydryl groups in tissue with Ellman's reagent. *Anal. Biochem.* **25:**192–205; 1968.
31. Laemmli, U. K. Cleavage of structural proteins during assembly of the head of bacteriophage T4. *Nature* **227:**680–685; 1970.
32. Bartosz, G.; Gaczynska, M. Effect of proteolysis on the electron spin resonance spectra of maleimide spin labeled erythrocyte membranes. *Biochim. Biophys. Acta* **821:**175–178; 1985.
33. Butterfield, D. A. Spin labeling in disease. *Biol. Magn. Reson.* **4:**1–78; 1982.
34. Hensley, K.; Postlewaite, J.; Dobbs, P.; Butterfield, D. A. Alteration of the erythrocyte membrane via enzymatic degradation of ankyrin (band 2.1): Subcellular surgery characterized by EPR spectroscopy. *Biochim. Biophys. Acta* **1145:**205–211; 1993.
35. Wyse, J. W.; Barker, R.; Franko, J. R.; Martelo, O.; Butterfield, D. A. Electron spin resonance studies of skeletal protein interactions in human erythrocyte membranes exposed to polyanions and in membranes prepared from inositol hexaphosphate-incorporated low-affinity erythrocytes. *Biochem. Biophys. Res. Commun.* **144:**779–786; 1987.
36. Farmer, B. T.; Harmon, T. M.; Butterfield, D. A. ESR studies of the erythrocyte membrane skeleton protein network: Influence of the state of aggregation of spectrin on the physical state of membrane proteins, bilayer lipids, and cell surface glycoproteins. *Biochim. Biophys. Acta* **821:**420–430; 1985.
37. Wyse, J.; Butterfield, D. A. Electron spin resonance and biochemical studies of the interaction of the polyamine, spermine, with the skeletal network of protein in human erythrocyte membranes. *Biochim. Biophys. Acta* **941:**141–149; 1988.
38. Butterfield, D. A.; Hensley, K.; Hall, N.; Umhauer, S.; Carney, J. Interaction of tacrine and velnacrine with neocortical synaptosomal membranes: Relevance to Alzheimer's disease. *Neurochem. Res.* **18:**989–994; 1993.
39. Butterfield, D. A.; Carney, J.; Umhauer, S.; Isbell, D.; Hall, N.; Hensley, K.; Rangachari, A. Changes in membrane cytoskeletal protein-protein interactions upon interaction of potential Alzheimer's disease therapeutic agents, in Alzheimer's disease. In: Corain, B., et al., eds. *Advances in clinical and basic research.* New York: Wiley Press; 1993:333–340.
40. Butterfield, D. A.; Rangachari, A. Membrane altering effects of velnacrine and N-methylacridinium: Relevance to tacrine and Alzheimer's disease. *Biochem. Biophys. Res. Commun.* **185:**596–603; 1992.
41. Nordio, P. L. General magnetic resonance theory. In: Berliner, L. J., ed. *Spin labeling, theory and applications.* New York: Academic Press; 1976:29–35.
42. Hubbell, W. L.; McConnell, H. M. Molecular motion in spin-labeled phospholipids and membranes. *J. Am. Chem. Soc.* **93:**314–323; 1971.
43. Youdim, M. B. H; Green, A. R. Iron deficiency and neurotransmitter synthesis and function. *Proc. Nutr. Soc.* **37:**173–179; 1978.

44. Dallman, P. R.; Simes, M. A.; Manies, E. L. Brain iron: Persistent deficiency following short-term iron deprivation in the young brain. *Br. J. Haematol.* **31**:209–215; 1975.
45. Gutteridge, J. M. C. Iron and oxygen radicals in brain. *Ann. Neurol. Supp.* **32**:S16–S21; 1992.
46. Tanaka, S. Isolation and characterization of protein kinase C from rat brain synaptosome cytoskeleton. *Kobe J. Med. Sci.* **37**:147–161; 1991.
47. Ptitsyn, O. B.; Semisotnov, G. V. The mechanism of protein folding. In: Nall, B. T.; Dill, K. A., eds. *Conformations and forces in protein folding.* Washington, DC: Amer. Assoc. Adv. Sci. 155–168; 1991.
48. Seppi C.; Castellana, A. M.; Minetti, G.; Piccinini, G.; Balduini, C.; Brovelli, A. Evidence for membrane protein oxidation during in vivo aging of human erythrocytes. *Mech. Ageing Dev.* **57**:247–258; 1991.
49. Castellana, M. A.; Piccinini, G.; Minetti, G.; Seppi, C.; Balduini, C.; Brovelli, A. Oxidation of membrane proteins and functional activity of band 3 in human red cell senescence. *Arch. Gerontol. Geriatr.* suppl. **3**:101–110; 1992.
50. Butterfield, D. A.; Nicholas, M. N.; Markesberry, W. R. Evidence for an increased rate of choline efflux across erythrocyte membranes in Alzheimer's disease. *Neurochem. Res.* **10**:909–918; 1985.
51. Kay, M. M. B. Band 3 in ageing and neurological disease. *Ann. New York Acad. Sci.* **621**:179–203; 1991.
52. Bosman, G. J. C. G. M.; Bartoleomeus, I. G. P.; DeMan, A. J. M.; Van Kalmthout, P. J. C.; DeGrip, W. J. Erythrocyte membrane characteristics indicate abnormal cellular ageing in patients with Alzheimer's disease. *Neurobiol. Ageing* **12**:13–18; 1991.
53. Katzman, R.; Saitoh, T. Advances in Alzheimer's disease. *FASEB J.* **5**:278–286; 1991.
54. Wischik, C. M.; Harrington, C. R.; Mudaetgova-Ladinska, E. B.; Novak, M.; Edwards, P. C.; McArthur, F. K. Molecular characterization and measurement of Alzheimer's disease pathology: Implications for genetic and environmental aetiology. *Ciba Found. Symp.* **169**:268–293; 1992.
55. Hensley, K.; Carney, J. M.; Aksenova, M.; Harris, M.; Wu, J. F.; Floyd, R.; Butterfield, D. A. A new model for β-amyloid aggregation and neurotoxicity based on free radical generation by the peptide: Relevance to Alzheimer's disease. *Proc. Natl. Acad. Sci. USA* **91**:3270–3274; 1994.